DOI: 10.1002/anie.201306328

Plasma Membrane Organization

High-Fidelity Protein Targeting into Membrane Lipid Microdomains in Living Cells**

*Oliver Beutel, Jörg Nikolaus, Oliver Birkholz, Changjiang You, Thomas Schmidt, Andreas Herrmann, and Jacob Piehler**

Abstract: *Lipid analogues carrying three nitrilotriacetic acid (tris-NTA) head groups were developed for the selective targeting of His-tagged proteins into liquid ordered (l_o) or liquid disordered (l_d) lipid phases. Strong partitioning into the l_o phase of His-tagged proteins bound to tris-NTA conjugated to saturated alkyl chains (tris-NTA DODA) was achieved, while tris-NTA conjugated to an unsaturated alkyl chain (tris-NTA SOA) predominantly resided in the l_d phase. Interestingly, His-tag-mediated lipid crosslinking turned out to be required for efficient targeting into the l_o phase by tris-NTA DODA. Robust partitioning into l_o phases was confirmed by using viral lipid mixtures and giant plasma membrane vesicles. Moreover, efficient protein targeting into l_o and l_d domains within the plasma membrane of living cells was demonstrated by single-molecule tracking, thus establishing a highly generic approach for exploring lipid microdomains in situ.*

The formation of membrane domains based on the separation of lipid mixtures into liquid-disordered (l_d) and liquid-ordered (l_o) phases has emerged as an important organizing principle of the plasma membranes of eukaryotic cells.[1] Submicroscopic l_o domains in the plasma membrane termed lipid rafts have been suggested to be involved in numerous cellular processes including signal transduction,[2] membrane-protein trafficking[3], and viral entry[4] and budding.[5] While the existence of a submicroscopic organization of lipids and proteins within the plasma membrane is well established, the particular properties of plasma membrane rafts and their functional roles in biological processes remain unclear.[6] Key challenges for unraveling the functional organization of lipid microdomains are the nanoscopic dimensions and the highly transient formation of l_o phases in the plasma membranes of living cells. While biochemical isolation of l_o phases from cells as "detergent-resistant membranes" is possible, this approach is not valid for exploring the intricate relationship between proteins and lipid rafts under native conditions.[7] To systematically explore the role of lipid phase separation for membrane protein function, versatile bioanalytical tools for selectively probing specific lipid microdomains and manipulating their proteins and lipids within living cells are required. We aimed to develop an approach for selectively and efficiently targeting proteins into distinct lipid phases of the plasma membranes of living cells, where they could be employed as sensors or actuators for exploring lipid microdomains. To this end, we synthesized multivalent chelator lipids based on a head group with three nitrilotriacetic acid (NTA) moieties grafted onto a cyclic scaffold to give tris-NTA, which has been demonstrated to bind His-tagged proteins with subnanomolar binding affinity.[8] For the targeting of proteins into l_d domains, a lipid-like anchoring group containing a single *cis* double bond was conjugated to tris-NTA (tris-NTA SOA,[9] Figure 1 a). Tris-NTA conjugated to a fully saturated lipid-like anchoring group (tris-NTA DODA, Figure 1 b) was employed for targeting into l_o phases. The partitioning of these lipids into lipid phases within artificial membranes was characterized quantitatively by using giant unilamellar vesicles (GUVs) and mica-supported membranes as model systems. After validating our approach, we used single-molecule tracking to investigate the targeting of proteins by tris-NTA SOA and tris-NTA DODA into submicroscopic lipid microdomains within the plasma membrane of living cells.

Efficient incorporation of tris-NTA DODA and tris-NTA SOA into lipid membranes and specific binding of His-tagged maltose binding protein (MBP) labeled with DY647 (^{DY647}MBP) was confirmed by probing binding to silica-supported membranes in real time using simultaneous total internal reflection fluorescence spectroscopy (TIRFS) and reflectance interference (RIf) detection.[10] To explore the potential role of binding stoichiometry, we tested His-tags with 6 (H6), 10 (H10), and 14 (H14) histidine residues. The tris-NTA head groups loaded with Ni^{II} ions provide coordination sites for six histidine residues and thus exactly match the H6 tag (Figure 1 c), while the H10 and H14 tags provide an excess of histidine residues. Rapid and stable binding of His-tagged MBPs to a 1,2-dioleoyl-*sn*-glycero-3-phosphocholine (DOPC) membrane doped with tris-NTA lipids loaded with Ni^{II} ions was confirmed, as was efficient elution with

[*] O. Beutel, O. Birkholz, Dr. C. You, Prof. Dr. J. Piehler
Division of Biophysics, Department of Biology
University of Osnabrück
Barbarastrasse 11, 49076 Osnabrück (Germany)
E-mail: piehler@uos.de
Homepage: http://www.biophysik.uni-osnabrueck.de
Dr. J. Nikolaus, Prof. Dr. A. Herrmann
Institute of Biology/Biophysics, Humboldt University
Berlin (Germany)
Prof. Dr. T. Schmidt
Physics of Life Processes, Leiden Institute of Physics (The Netherlands)

[**] We thank Gabriele Hikade and Hella Kenneweg for technical support. This project was supported by the Deutsche Forschungsgemeinschaft (NanoSciERA/PI405-4 and SFB 944 to J.P.; SFB 765 and GK 1171 to A.H.) and by the Foundation for Fundamental Research on Matter (part of the Netherlands Organisation for Scientific Research) to T.S. (NanoSciERA/06NSE02).

Supporting information for this article is available on the WWW under http://dx.doi.org/10.1002/anie.201306328.

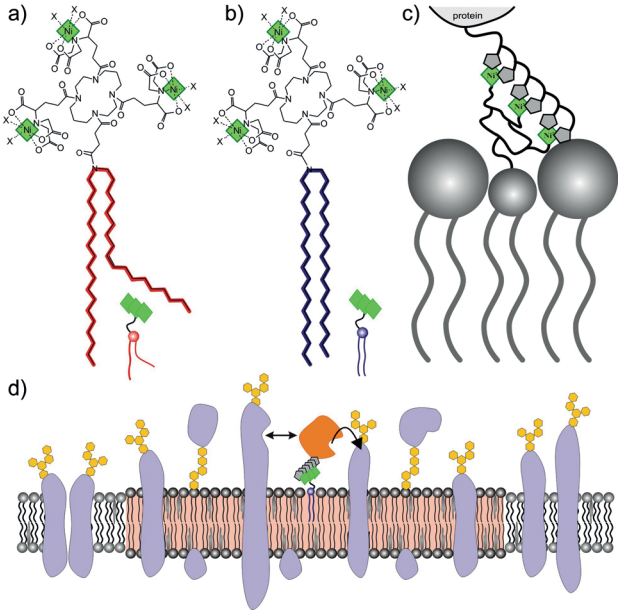

Figure 1. Tris-NTA lipids for the targeting of proteins into lipid microdomains. a, b) Chemical structures of tris-NTA SOA (a) and tris-NTA DODA (b). c) Tethering of His-tagged proteins to tris-NTA lipids within a membrane. d) Lipid-tethered proteins as tools for the selective activation or modification of other proteins within submicroscopic lipid domains of the plasma membrane, schematically depicted here as a lipid raft (pink background), targeted through tris-NTA DODA.

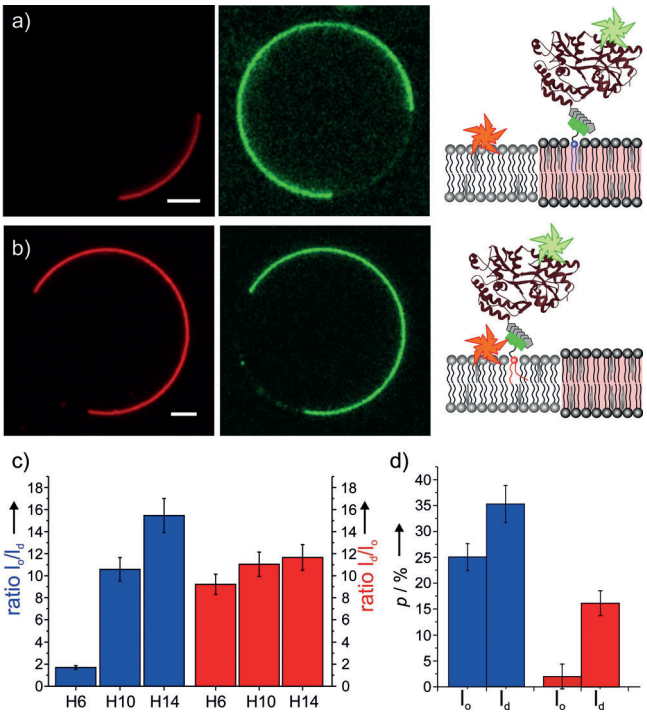

Figure 2. Partitioning of His-tagged MBP bound to tris-NTA lipids in phase-separating lipid membranes. a, b) ^{AF488}MBP-H10 (green channel) tethered to GUVs. RhoB-DOPE (red channel) was used as an l_d marker. a) tris-NTA DODA; b) tris-NTA SOA. Scale bar: 5 μm. c) Partitioning of MBP with His tags of different lengths bound to tris-NTA DODA (blue) or tris-NTA SOA (red). d) Binding probabilities *p* of a H6-tag-functionalized AFM tip with tris-NTA DODA (blue) and tris-NTA SOA (red) in l_o and l_d phases.

imidazole (Figure S1 in the Supporting Information). Binding amplitudes decreased with a decreasing fraction of tris-NTA lipids in the membrane, but stable protein binding was observed even at 0.25 mol% (Figure S2).

The partitioning of His-tagged MBP tethered to phase-separating membranes (cholesterol/sphingomyelin/DOPC 1:1:1 containing 1% tris-NTA lipid) was probed by using GUVs doped with 1,2-dioleoyl-*sn*-glycero-3-phosphoethanolamine-*N*-(lissamine rhodamine B sulfonyl) (rhodamine-DOPE) as a marker for the l_d phase. MPB-H10 labeled with Alexa Fluor 488 (^{AF488}MBP-H10) and bound to the surface of the GUVs through tris-NTA DODA was located mainly within l_o domains (Figure 2a), while nearly exclusive localization in the l_d domains was observed in GUVs doped with tris-NTA SOA (Figure 2b). Quantitative analysis revealed an l_o/l_d ratio of 10:1 for tris-NTA DODA and 1:25 for tris-NTA SOA. Efficient targeting of His-tagged proteins into the l_o and l_d domains was thus possible when using these tris-NTA lipids.

For more detailed studies of the targeting of proteins into lipid domains, solid-supported membranes on mica, which readily allow phase separation in micron-sized domains,[11] were employed. Efficient targeting of MBP-H10 into l_o and l_d domains by tris-NTA DODA and tris-NTA SOA, respectively, was confirmed by confocal and total internal reflection fluorescence (TIRF) imaging (Figure S3). Upon applying MBP with shorter and longer His tags, striking differences in phase partitioning were observed when using tris-NTA DODA. For MBP-H6, only an approximately two-fold higher concentration within the l_o phase was observed, while for MBP-H10, a much stronger partitioning of approximately ten-fold into the l_o phase was found. MBP-H14 showed an even more pronounced partitioning into the l_o phase compared to MBP-H10 (Figure 2c, Table S1). In GUVs, similar differences in the l_o phase partitioning of bound protein were confirmed (Figure S4). By contrast, no significant dependence on the length of the His tag was observed for partitioning mediated by tris-NTA SOA; in this case there was always approximately ten-fold enrichment of the His-tagged MBP within the l_d phase (Figure 2c and Figure S5, Table S1).

These observations suggested that the crosslinking of tris-NTA lipids mediated by longer His tags may induce partitioning of tris-NTA DODA into the l_o phase. Time-lapse experiments for protein binding to phase-separated membranes indeed indicated that partitioning of tris-NTA DODA occurred during protein binding (Figure S6). We therefore measured the distribution of tris-NTA DODA within l_o and l_d phases in the absence of His-tagged proteins by force spectroscopy with an H6 tag tethered to the surface of an AFM tip as a probe (Figure S7). Strikingly, similar numbers of binding events were observed for tris-NTA DODA in the l_o and l_d domains (Figure 2d). By contrast, strong (ca. eight-fold) enrichment of tris-NTA SOA within l_d domains was confirmed (Figure 2d), a result consistent with the observed partitioning of His-tagged proteins. The stronger partitioning of MBP-H10 and MBP-H14 compared to MBP-

H6 could be explained by simultaneous interaction with more than one tris-NTA DODA owing to an excess of His residues.[12] Such crosslinking of multiple tris-NTA moieties by the H10 and H14 tags was explored by probing the dissociation kinetics of His-tagged MBP upon injection of imidazole (100 mM).[13] The dissociation rate constants for H10 and H14 were lower by factors of 7 and 13, respectively, compared to MBP-H6 (Figure S8), thus corroborating binding to more than one tris-NTA head group. These results support the idea that lipid crosslinking is responsible for efficient partitioning of proteins bound to tris-NTA DODA into the l_o phase.

To evaluate these tris-NTA lipids as probes for submicroscopic membrane domains, we characterized their diffusion dynamics by single-molecule tracking. Homogeneous diffusion of individual His-tagged ^{DY647}MBP molecules tethered to mica-supported fluid DOPC membranes doped with tris-NTA lipids was observed (Video 1 and Figure S9). Very similar diffusion constants of approximately 1.3 $\mu m^2 s^{-1}$ were obtained for MBP-H6, MBP-H10, and MBP-H14 bound to tris-NTA SOA or tris-NTA DODA in homogeneous DOPC membranes (Figure S9 and Table S2), thus suggesting that the crosslinking induced by the longer tags does not significantly alter the diffusion properties. Within phase-separated membranes, characteristic differences in the diffusion of ^{DY647}MBP-H10 tethered to tris-NTA DODA or tris-NTA SOA were observed (Video 2 and Figure 3). Typical trajectory maps obtained for ^{DY647}MBP-H10 bound to tris-NTA DODA and tris-NTA SOA are shown in Figure 3a and b, respectively. The diffusion patterns confirm efficient targeting into the l_o and l_d domains on the single-molecule level. The strongly confined diffusion observed for ^{DY647}MBP-H10 bound to tris-NTA DODA was confirmed by a mean square displacement (MSD) analysis (Figure 3c). Confinement was also observed for ^{DY647}MBP-H10 bound to tris-NTA SOA, but to a much lower extent. Diffusion constants of (0.5 ± 0.1) $\mu m^2 s^{-1}$ and (1.1 ± 0.1) $\mu m^2 s^{-1}$ for ^{DY647}MBP-H10 bound to tris-NTA DODA and tris-NTA SOA, respectively, were obtained by fitting to a model for confined diffusion. The average domain sizes obtained from the fit (diameter: 1.3 μm for tris-NTA DODA and 3.2 μm for tris-NTA SOA) were in good agreement with the average domain sizes of l_o and l_d phases (1.2 μm and 2.9 μm, respectively). These results clearly established that the diffusion kinetics could be employed as a readout for successful targeting of proteins into the l_d and l_o phases.

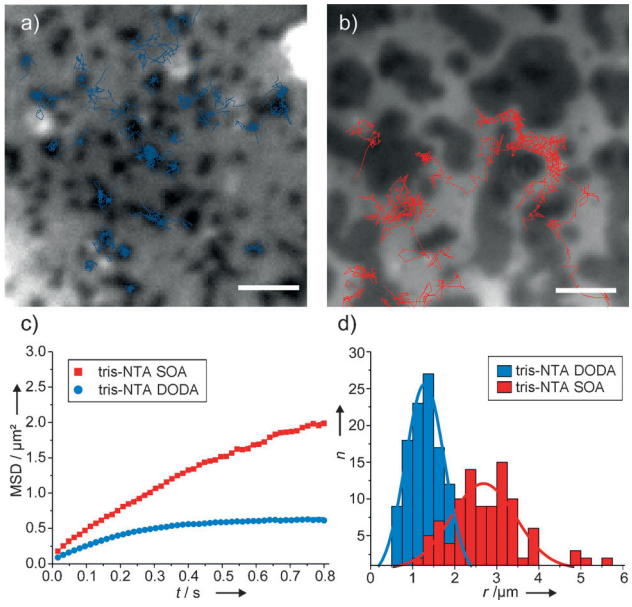

Figure 3. Diffusion of ^{DY647}MBP-H10 targeted into different lipid phases. a, b) Trajectories from individual ^{DY647}MBP-H10 molecules bound to tris-NTA DODA (a) or tris-NTA SOA (b). Scale bar: 5 μm. c) Mean square displacement (MSD) analyses from the experiments shown in panel a (blue) and panel b (red). d) Histogram of domain sizes obtained from confined diffusion analysis.

Having demonstrated the ability to efficiently bind, target, and track individual proteins within l_o and l_d phases in artificial membranes, we explored the partitioning of tris-NTA lipids within natural phase-separating lipid mixtures. Efficient lipid domain targeting of MBP-H10 by tris-NTA lipids was confirmed for GUVs prepared from influenza virus lipids (Figure S10 and Table 1). In giant plasma membrane vesicles (GPMVs) obtained from HeLa cells (Figure S11), similar partitioning properties (83% in the l_o phase by tris-NTA DODA and 85% in the l_d phase by tris-NTA SOA) were observed (Table 1).

Table 1: Partitioning of labeled MBP-H10 bound to tris-NTA DODA and tris-NTA SOA.

Lipid system	Tris-NTA DODA[a]	Tris-NTA SOA[b]
GUV/synthetic[c]	13 ± 4	12 ± 2
Mica/synthetic[d]	12 ± 2	14 ± 2
GUV/viral[e]	6 ± 2	7 ± 2
GPMV/HeLa	5 ± 2	6 ± 2

[a] Partitioning ratio $l_o \backslash l_d$. [b] Partitioning ratio $l_d \backslash l_o$. [c] Mixture (DOPC\cholesterol\C18:0 sphingomyelin). [d] Mixture (DOPC\cholesterol\brain sphingomyelin). [e] GUVs prepared from influenza virus lipids.

The key role of His-tag length in the l_o-phase partitioning of MBP tethered to tris-NTA DODA, but not in the l_d-phase partitioning of MBP tethered to tris-NTA SOA, was also confirmed in GPMVs (Table S3). Moreover, very similar partitioning in GUVs and GPMVs was observed for the HaloTag protein fused to H6 or H12, respectively (Figures S12, S13 and Table S3).

We therefore explored the targeting of proteins into lipid domains within the plasma membrane of living cells. After loading the plasma membranes of live HeLa cells with either tris-NTA DODA or tris-NTA SOA, specific binding of ^{DY647}MBP-H10 was observed (Figure S14), and this binding could be reversed by the addition of imidazole. Tracking ^{DY647}MBP-H10 in the membranes of HeLa cells identified highly characteristic differences (Video 3 and Figure 4): in the case of tris-NTA SOA, the MSD analysis revealed fast, nearly free diffusion on the plasma membrane. By contrast, the diffusion of ^{DY647}MBP-H10 bound to tris-NTA DODA was strongly confined (Figure 4c) and significantly slower compared to that bound to tris-NTA SOA (Figure 4d). As the time resolution employed in these experiments cannot resolve

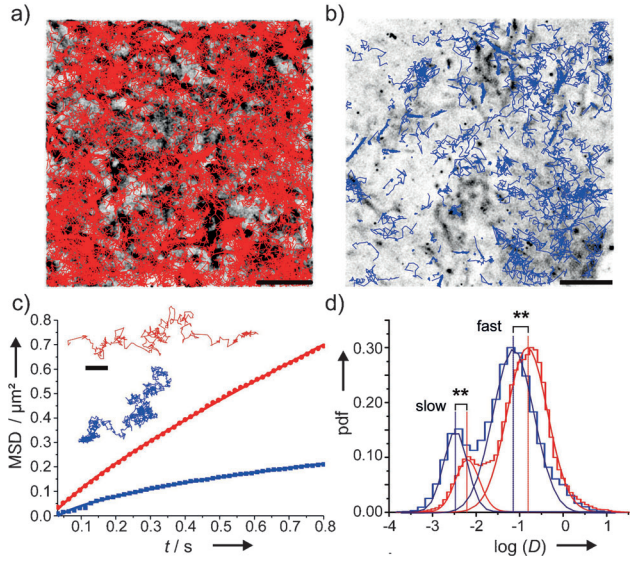

Figure 4. Diffusion properties of ^{DY647}MBP-H10 bound to tris-NTA lipids in living cells. a,b) Trajectories of individual ^{DY647}MBP-H10 molecules bound to tris-NTA SOA (a) or tris-NTA DODA (b) inserted into the plasma membranes of HeLa cells, plotted from a 300-frame time lapse sequence. A similar total number of steps are shown for each for easier comparison. Scale bar: 5 µm. c) MSD analyses for trajectories from tris-NTA SOA (red) or tris-NTA DODA (blue). Typical trajectories with a similar number of steps are shown in the inset (scale bar: 1 µm). d) Probability density function (pdf) of local diffusion constants (*D*) obtained from a step-length analysis of the first 5 steps. The average fast and slow diffusion constants obtained from a bimodal fit are indicated.

diffusion within lipid rafts, we explain this apparent confinement by dynamic trapping within such submicroscopic domains. While similar diffusion properties were observed for ^{DY647}MBP-H14 bound to tris-NTA DODA, much less apparent confinement was observed for ^{DY647}MBP-H6 (Figure S15, Table S4). By contrast, the diffusion properties of proteins tethered to the plasma membrane through tris-NTA SOA did not depend on the length of the His tag (Figure S13). These diffusion properties of MBP-H10 tethered to tris-NTA lipids in the plasma membrane are in very good agreement with previously investigated l_d and l_o probes (Table S5).

More detailed insight into the spatiotemporal organization of MBP-H10 tethered to the membrane through tris-NTA lipids was obtained by treatment with drugs for altering the properties of membrane microdomains (Figure S16). While in the case of tris-NTA SOA, the diffusion properties were only affected by destabilization of the actin-based membrane skeleton, cholesterol depletion dramatically reduced mobility in case of tris-NTA DODA. These observations are in agreement with previous studies on the role of cholesterol in the diffusion of glycosylphosphatidylinositol (GPI)-anchored proteins,[14] which are believed to partition into lipid rafts.[15] These results clearly corroborate the idea that efficient targeting of proteins into submicroscopic l_o and l_d domains within the plasma membrane is possible through tris-NTA DODA and tris-NTA SOA, respectively.

In conclusion, we have developed generic tools for efficiently tethering proteins to l_o and l_d phases with very high specificity. This method was demonstrated to work very reliably in the plasma membranes of living cells, thus allowing the targeting of exogenously applied proteins into lipid rafts with high specificity. Compared to reported l_o probes,[6c] tris-NTA DODA in combination with a protein or peptide capable of dimerizing the tris-NTA through a histidine tag of ten or more residues turned out to be considerably more efficient and robust even in the case of the phase-separated membranes formed by natural lipid mixtures. This behavior can probably be attributed to the fact that dimerization-based partitioning is based on differences in the translational entropy of lipids within the l_o and l_d phases, which is independent of the lipid composition. By contrast, traditional l_o probes are designed based on enthalpy (and conformational entropy) aspects, which are highly dependent on the specific molecular structures of the lipids within the l_d and l_o phases. In line with this argument, dimerization of (palmitoylated) receptors and GPI-anchored proteins has frequently been observed to drive partitioning into lipid rafts.[16] Moreover, the most reliable l_o probe is cholera toxin B, which also crosslinks several lipids and yields similar partitioning efficiencies to those observed for MBP-H10 bound to tris-NTA DODA.[16b] Tris-NTA lipids thus also provided a simple experimental basis for highlighting the key relevance of dimerization for l_o partitioning.

These potent functional properties of tris-NTA lipids enable the rapid induction of protein activity at the plasma membrane in a spatially and temporally controlled manner. For proof-of-concept experiments, we have here employed an indifferent protein labeled with a photostable fluorescent dye for confirming successful lipid phase targeting. However, the wide spectrum of available protein activities could be exploited by this approach to develop novel bioanalytical tools for exploring the lipid-phase-based compositional and functional mosaicity of the plasma membrane. Proteases or biotin ligases could be employed for identifying proteins association with lipid microdomains. Moreover, the substrates for certain plasma membrane machineries could be specifically targeted into microdomains to unravel the functional implications of lipid phase separation. The tris-NTA lipids developed in this study provide ideal properties for this purpose: in order to control exposure times, rapid, high-affinity tethering in situ is achieved through the tris-NTA–oligohistidine interaction, and rapid elution with imidazole quenches protein functions without affecting cell viability. As many recombinant proteins are produced with a His tag, highly generic application is ensured. Most importantly, multivalent binding allows efficient, high-affinity tethering even at low levels of doping with chelator lipids, a property essential for application in live cells. By contrast, traditional monovalent NTA lipids, which have been successfully applied for the targeting of proteins to l_o phases in vitro,[17] are not suitable for this purpose since they bind efficiently only at relatively high doping levels (≥ 10 mol %).[18] The highly efficient targeting of protein-based sensors and actuators to either l_o or l_d domains by tris-NTA DODA and tris-NTA SOA, respectively, ensures low background and the opportunity for robust control experiments.

Received: July 20, 2013
Revised: October 4, 2013
Published online: December 18, 2013

Keywords: lipid-phase separation · lipid rafts · multivalent chelators · proteins · single-molecule studies

[1] a) K. Simons, E. Ikonen, *Nature* **1997**, *387*, 569 – 572; b) S. Mayor, M. Rao, *Traffic* **2004**, *5*, 231 – 240; c) P. F. Lenne, L. Wawrezinieck, F. Conchonaud, O. Wurtz, A. Boned, X. J. Guo, H. Rigneault, H. T. He, D. Marguet, *EMBO J.* **2006**, *25*, 3245 – 3256; d) D. Lingwood, K. Simons, *Science* **2010**, *327*, 46 – 50; e) A. Kusumi, T. K. Fujiwara, N. Morone, K. J. Yoshida, R. Chadda, M. Xie, R. S. Kasai, K. G. Suzuki, *Semin. Cell Dev. Biol.* **2012**, *23*, 126 – 144.

[2] a) K. G. Suzuki, R. S. Kasai, K. M. Hirosawa, Y. L. Nemoto, M. Ishibashi, Y. Miwa, T. K. Fujiwara, A. Kusumi, *Nat. Chem. Biol.* **2012**, *8*, 774 – 783; b) A. D. Douglass, R. D. Vale, *Cell* **2005**, *121*, 937 – 950; c) Y. Kaizuka, A. D. Douglass, S. Vardhana, M. L. Dustin, R. D. Vale, *J. Cell Biol.* **2009**, *185*, 521 – 534; d) T. Zech, C. S. Ejsing, K. Gaus, B. de Wet, A. Shevchenko, K. Simons, T. Harder, *EMBO J.* **2009**, *28*, 466 – 476; e) R. Lasserre, X. J. Guo, F. Conchonaud, Y. Hamon, O. Hawchar, A. M. Bernard, S. M. Soudja, P. F. Lenne, H. Rigneault, D. Olive, G. Bismuth, J. A. Nunes, B. Payrastre, D. Marguet, H. T. He, *Nat. Chem. Biol.* **2008**, *4*, 538 – 547.

[3] R. W. Klemm, C. S. Ejsing, M. A. Surma, H. J. Kaiser, M. J. Gerl, J. L. Sampaio, Q. de Robillard, C. Ferguson, T. J. Proszynski, A. Shevchenko, K. Simons, *J. Cell Biol.* **2009**, *185*, 601 – 612.

[4] a) P. Scheiffele, M. G. Roth, K. Simons, *EMBO J.* **1997**, *16*, 5501 – 5508; b) U. Coskun, K. Simons, *FEBS Lett.* **2010**, *584*, 1685 – 1693.

[5] a) L. A. Carlson, J. H. Hurley, *Proc. Natl. Acad. Sci. USA* **2012**, *109*, 16928 – 16933; b) B. Brugger, B. Glass, P. Haberkant, I. Leibrecht, F. T. Wieland, H. G. Krausslich, *Proc. Natl. Acad. Sci. USA* **2006**, *103*, 2641 – 2646.

[6] a) K. Simons, M. J. Gerl, *Nat. Rev. Mol. Cell Biol.* **2010**, *11*, 688 – 699; b) P. J. Quinn, *Prog. Lipid Res.* **2010**, *49*, 390 – 406; c) E. Sezgin, I. Levental, M. Grzybek, G. Schwarzmann, V. Mueller, A. Honigmann, V. N. Belov, C. Eggeling, U. Coskun, K. Simons, P. Schwille, *Biochim. Biophys. Acta Biomembr.* **2012**, *1818*, 1777 – 1784.

[7] D. Lichtenberg, F. M. Goni, H. Heerklotz, *Trends Biochem. Sci.* **2005**, *30*, 430 – 436.

[8] S. Lata, A. Reichel, R. Brock, R. Tampé, J. Piehler, *J. Am. Chem. Soc.* **2005**, *127*, 10205 – 10215.

[9] S. Lata, M. Gavutis, J. Piehler, *J. Am. Chem. Soc.* **2006**, *128*, 6 – 7.

[10] M. Gavutis, S. Lata, P. Lamken, P. Müller, J. Piehler, *Biophys. J.* **2005**, *88*, 4289 – 4302.

[11] J. Ries, S. Chiantia, P. Schwille, *Biophys. J.* **2009**, *96*, 1999 – 2008.

[12] A. Reichel, D. Schaible, N. Al Furoukh, M. Cohen, G. Schreiber, J. Piehler, *Anal. Chem.* **2007**, *79*, 8590 – 8600.

[13] S. Lata, J. Piehler, *Anal. Chem.* **2005**, *77*, 1096 – 1105.

[14] a) M. Vrljic, S. Y. Nishimura, W. E. Moerner, H. M. McConnell, *Biophys. J.* **2005**, *88*, 334 – 347; b) S. Y. Nishimura, M. Vrljic, L. O. Klein, H. M. McConnell, W. E. Moerner, *Biophys. J.* **2006**, *90*, 927 – 938; c) F. Pinaud, X. Michalet, G. Iyer, E. Margeat, H. P. Moore, S. Weiss, *Traffic* **2009**, *10*, 691 – 712.

[15] I. Levental, M. Grzybek, K. Simons, *Biochemistry* **2010**, *49*, 6305 – 6316.

[16] a) O. Cunningham, A. Andolfo, M. L. Santovito, L. Iuzzolino, F. Blasi, N. Sidenius, *EMBO J.* **2003**, *22*, 5994 – 6003; b) I. Levental, D. Lingwood, M. Grzybek, U. Coskun, K. Simons, *Proc. Natl. Acad. Sci. USA* **2010**, *107*, 22050 – 22054; c) S. Paladino, D. Sarnataro, R. Pillich, S. Tivodar, L. Nitsch, C. Zurzolo, *J. Cell Biol.* **2004**, *167*, 699 – 709.

[17] J. C. Stachowiak, C. C. Hayden, M. A. Sanchez, J. Wang, B. C. Bunker, J. A. Voigt, D. Y. Sasaki, *Langmuir* **2011**, *27*, 1457 – 1462.

[18] I. T. Dorn, K. R. Neumaier, R. Tampe, *J. Am. Chem. Soc.* **1998**, *120*, 2753 – 2763.

